Lipidome analysis of breast milk composition in humans, monkeys, bovids, and pigs.

Aleksandra Mitina
Skolkovo Institute of Science and Technology
Pavel Mazin
Skolkovo Institute of Science and Technology
Anna Vanyushkina
Skolkovo Institute of Science and Technology
Nikolay Anikanov
Skolkovo Institute of Science and Technology
Waltraud Mair
Skolkovo Institute of Science and Technology
Song Guo
Skolkovo Institute of Science and Technology
philipp khaitovich (khaitovich@eva.mpg.de)
Skolkovo Institute of Science and Technology

Research article

Keywords: lipidome, breast milk, evolution

Posted Date: December 19th, 2019

DOI: https://doi.org/10.21203/rs.2.19305/v1

Version of Record: A version of this preprint was published on June 19th, 2020. See the published version at https://doi.org/10.1186/s12862-020-01637-0.

Abstract

Background Lipids contained in breast milk are an essential source of energy and structural materials for a growing infant. Furthermore, lipids' long-chain unsaturated fatty acid residues can directly participate in infant tissue formation. Here, we used untargeted mass spectrometric measurements to assess breast milk lipid composition in seven mammalian species: humans, two macaque species, cows, goats, yaks, and pigs.

Results Analysis of the main milk lipid class, triacylglycerides, revealed species-specific differences in the composition of fatty acid residues for each of seven species. While human milk showed more medium and long-chain unsaturated fatty acids, pig milk composition was the most distinct, featuring the highest proportion of long-chain polyunsaturated fatty acids.

Conclusions We show that breast milk lipidome composition is dynamic across mammalian species, changed extensively in pigs, and contains features particular to humans.

Background

Breast milk is the sole source of nutrients for the infant's growth and development. Accordingly, breast milk must contain adequate proportions of all nutrients required for the infant's growth [1, 2]. These requirements differ among species due to ecological and biological variability of infants' development, mirrored by the variation in breast milk composition [3]. Besides nutritional components, breast milk contains steroid and peptide hormones including leptin, ghrelin, and adiponectin [4], immune and growth factors [2, 5, 6], as well as poly-unsaturated fatty acids directly participating in the infant tissue development and growth [7, 8].

The most variable element of breast milk composition is total fat content ranging from 60% in the hooded seals [9] to less than 1% in white rhinoceroses and ring-tailed lemur [10] – the phenomenon mainly linked to the duration of breastfeeding and ecological conditions. In most species, however, a single lipid class, triacylglycerides (TAGs), composes on average, 98% of the milk fat [11]. TAGs have simple chemical composition, consisting of glycerol and three fatty acid residues. Several studies analyzed breast milk TAG composition in mammalian species, including humans [12–16], demonstrating differences in the distribution of DHA-containing TAGs in comparison with the baby formula [17]. However, the systematic characterization of the breast milk lipidome composition across mammalian species remained incomplete.

While most lipids contained in breast milk get broken down to energy sources and simple building blocks, there is evidence that some of TAG fatty acid residues could directly participate in infant tissue development and growth. For example, docosahexaenoic acid (DHA) derived from milk TAGs is transported across the blood-brain barrier in the form of LPC with the help of a specific protein transporter [18]. The direct use of milk fatty acid residues in infant tissue development indicates that breast milk lipidome composition of a species might reflect specific requirements of its infant tissues. To approach

this question, we first assessed the extent of breast milk TAG composition differences among seven mammalian species, including humans represented by two distinct populations.

Results

We examined lipid composition of breast milk samples from healthy human volunteers representing Russian (Moscow) and Chinese (Shanghai) populations (n = 20), cows (n = 4), goats (n = 4), pigs (n = 4), domestic yaks (n = 2), rhesus monkeys (n = 2), and crab-eating monkeys (n = 2) (Additional file 5: Table S1). Furthermore, for each species, we measured a pooled sample containing equal volumes of milk from each individual.

Phylogenetically, examined species represent two orders of mammals: artiodactyla, or cloven-hoofed mammals, and primate. Within artiodactyla, our study contains representatives of two families: suidae (pig) and bovidae (cow, domestic yak, and goat). Primate species were represented by cercopithecidae (crab-eating and rhesus monkeys) and hominidae (human) (Fig. 1A).

Randomized milk samples were extracted, separated using liquid chromatography, and measured using untargeted mass spectrometry in positive ionization mode. The measurements yielded a total of 472 mass spectrometry features representing distinct hydrophobic compounds (lipids) with molecular weights below 1,200 Daltons (Da).

Visualization of the relationship among samples based on the abundance levels of these 472 detected lipids using multidimensional scaling (MDS) revealed good separation of species and phylogenetic groups (Fig. 1B). Furthermore, distances between species calculated using the normalized intensities of mass spectrometry signals generally agreed with the phylogenetic distances (Fig. 1C). Pig milk was the only obvious exception from this linear relationship, showing a greater difference to the bovidae species than expected from the phylogeny.

Of the 472 detected lipids 403 (85%) showed significant intensity differences among species (ANOVA, BH-corrected $P < 0.05$). Unsupervised clustering of these 403 species-dependent lipids based on their intensity profiles across samples yielded four clusters (Fig. 2A). Notably, lipid intensities within these clusters differed within the mammalian orders as much as between them. Particularly, the lipid composition of the pig milk stood out in three of the four clusters, while cluster 4 contained milk lipidome composition features shared between monkeys and bovids (Fig. 2B).

In agreement with previous knowledge, of all lipids detected in milk, the most of lipid was covered by a specific lipid class – triacylglycerides (TAGs). Interestingly, 76 lipid features computationally annotated as TAGs were present in all four clusters, covering the entire spectrum of lipid variation patterns (Additional file 6: Table S2). Furthermore, the average length and unsaturation extent of the fatty acid chains of these TAGs deferred among the clusters (Fig. 2C). For instance, cluster 2 TAGs contained long-chain polyunsaturated fatty acid residues, while cluster 4 TAGs preferentially contained medium-chain fatty acid residues (Fig. 2C; Additional file 1: Figure S1).

Notably, relative abundance analysis of detected TAGs revealed apparent intensity differences characteristic of each species. Specifically, cow milk contained more TAGs composed of long monounsaturated fatty acids. By contrast, goat milk contained more TAGs composed of medium-chain saturated and monounsaturated fatty acids. Pigs milk stood out from the rest of the species by having TAGs composed of long- and very long-chain polyunsaturated fatty acids. Monkey milk had more TAGs composed of medium-chain monounsaturated and polyunsaturated fatty acids. Finally, human milk tended to contain more TAGs with long-chain polyunsaturated fatty acids (Fig. 3A; Additional file 1: Figure S1).

We next specifically searched for lipids showing statistically significant intensity differences between humans and other three species' groups represented in our study. Of the 472 detected lipids, 94 differed in intensity between humans and macaques, 23 of them annotated as TAGs (ANOVA, BH-corrected $P < 0.05$). Clustering of these lipids revealed a notable intensity increase in the human milk for a group of lipids, including nine TAGs with long- and very long-chain fatty acids (Fig. 4; Additional file 2: Figure S2).

Comparison between humans and bovids yielded significant intensity differences for 269 lipids, 61 of them annotated as TAGs (ANOVA, BH-corrected $P < 0.05$). Among them, 23 TAGs with long- and very long-chain polyunsaturated fatty acids showed increased intensities in human milk (Fig. 5B; Additional file 3: Figure S3).

Comparison between humans and pigs revealed significant intensity differences for 343 lipids, 64 of them annotated as TAGs (ANOVA, BH-corrected $P < 0.05$). Among them, 15 TAGs containing medium-chain saturated, monounsaturated, and polyunsaturated fatty acids were increased in the human milk, while the rest of TAGs containing long- and very long-chain polyunsaturated fatty acids were elevated in the pig milk (Fig. 4C; Additional file 4: Figure S4).

Discussion

We show that triacylglycerides, the main components of the milk fat, differ widely among mammalian species in terms of their average fatty acid length and unsaturation degree. Of the seven species examined in our study, pig milk shows the most rapid evolutionary divergence, resulting in unusually high proportion of polyunsaturated fatty acids. This rapid evolution might either represent the relaxation of stabilizing selection or, more likely, an adaptive change enabling shortening of the lactation period on the suidae lineage.

Importantly, we detect specific features of the breast milk lipidome composition in each of the seven species, including humans. While we were unable to obtain milk samples from apes, the comparison to two old world monkey species, rhesus and crab-eating macaques, revealed breast milk lipidome features potentially unique to humans. Specifically, we show that after the human-monkey species' divergence approximately 30 million years ago, human ancestors started to produce milk with higher abundance of TAGs containing long-chain fatty acids with high levels of unsaturation. This observation is intriguing, given the reports of particular long-chain poly-unsaturated fatty acids accumulating in the human brain

during the last trimester of pregnancy and after birth [19] potentially influencing brain development and functionality [8]. In addition to TAGs, we detect human-specific intensity differences for lipids representing other lipid classes present in milk, such as phospholipids. However, given the small sample size of the study, we did not consider low-abundance lipid classes in our analysis.

Conclusions

Our study revealed substantial differences in triacylglyceride composition among seven mammalian species: three primates, three bovids, and pigs. While for most species changes in milk lipidome composition fit the general evolutionary pattern, with distances proportional to the phylogenetic times, there is an exception. Specifically, pig milk stood out by containing unusually high amounts of long-chain polyunsaturated fatty acids. Notably, human milk was second in terms of long-chain polyunsaturated fatty acids abundance, followed by two macaque species, and then by the bovids. These results indicate the need for further studies of breast milk lipidome evolution in conjunction with other developing tissues, especially the brain.

Methods

Sample collection

We collected breast milk samples from human volunteers of Russian and Chinese descend (10 samples each), cows (four samples), goats (four samples), pigs (four samples), yaks (two samples), rhesus monkeys (two samples), and crab-eating monkeys (two samples). Informed consent for the use of milk in this study was obtained from each of the human volunteers. A written permission was obtained from animal owners upon collecting animal milk samples. In all species, milk samples were collected at matched lactation stage, several weeks after infants' birth. In each case, milk was sampled at the end of breastfeeding or milking event into the same type of 10-ml plastic container and immediately placed into − 20 °C freezer for short-term storage not exceeding two weeks. Samples were then transported on dry ice without de-freezing into − 80 °C freezer for long-term storage, not exceeding four months.

Ethic statement

All animals were treated in accordance with good animal practice as defined by the local welfare authorities; all human volunteers have signed an Informed Consent Form, confirming that they understand the purpose of the research and their participation is entirely gratuitous.

Lipid extraction

The milk aliquots were thawed at 0 °C mixed, and 16 µl of milk were transferred to a 2.0 ml Eppendorf safe-lock tube and resuspended in 34 µl of LC-MS grade water. Prior to extraction, samples were randomized with regard to species' identity. For lipid extraction, a modified two-phase protocol was used as described in [20]. All manipulations with samples were performed on ice. Briefly, 750 µl of MeOH:MTBE (1:3) solution containing internal standards in concentration of 1 mg/L were added to each sample,

vortexed for 1 min, sonicated for 15 min in an ice-cooled sonication bath, incubated for 30 min at 4 °C, and sonicated for the second time in a pre-cooled sonication bath. Then, 560 µl of MeOH:H2O (1:3) solution was added to each sample, vortexed for 10 sec and centrifuged for 10 min at 14.000 x g at 4 °C. The 400 µl of the upper-phase, containing organic fraction, was transferred to a new 2.0 ml Eppendorf tube and dried in a Speedvac for 1 h at 30 °C.

Mass-spectrometry

Dried lipid pellets were resuspended in 400 µl of acetonitrile:isopropanol (1:3) solution. Samples were rigorously vortexed for 10 sec, shaken for 10 min at 4°C and sonicated in an ice bath. Then, 5 µl of each sample was transferred to the autosampler glass vial and diluted 1:20 with 95 µl of acetonitrile:isopropanol (1:3) solution. A pool of all samples was prepared by mixing 5 µl from each sample in a separate Eppendorf tube, transferred to glass vials and diluted 1:20 with acetonitrile:isopropanol (1:3) solution to get quality control (QC) samples. Sample pools for each species were made by mixing 10 µl of each sample of the corresponding species and diluted 1:20 with acetonitrile:isopropanol (1:3) solution. From each diluted sample, 3 µl were injected to a reversed-phase Bridged Ethylene Hybrid (BEH) C8 reverse column (100 mm x 2.1 mm, containing 1.7 µm diameter particles, Waters) coupled to a Vanguard pre-column with the same dimensions, using a Waters Acquity UPLC system (Waters, Manchester, UK). The mobile phases used for the chromatographic separation were: water, containing 10 mM ammonium acetate, 0.1% formic acid (Buffer A) and acetonitrile:isopropanol (7:3 (v:v)), containing 10 mM ammonium acetate, 0.1% formic acid (Buffer B). The gradient separation was: 1 min 55% B, 3 min linear gradient from 55% to 80% B, 8 min linear gradient from 80% B to 85% B, and 3 min linear gradient from 85% A to 100% A. After 4.5 min washing with 100% B the column was re-equilibrated with 55% B. The flow rate was set to 400 µl/min. The mass spectra were acquired in a positive mode using a heated electrospray ionization source in combination with a Bruker Impact II QTOF (quadrupole-Time-of-Flight) mass spectrometer (Bruker Daltonics, Bremen, Germany).

Four blank samples were run at the beginning of the queue, followed by four QC samples to equilibrate the column. After them, 38 samples were queued in the same random order used for extraction with all samples randomized by species, interleaved with seven pooled samples, one QC preceding the first sample and then a QCs after every 9th sample. At the end of the queue, we performed two injections containing 100% acetonitrile to wash the column, followed by blank samples. Blank samples were prepared as usual samples, but contained only extraction buffers to reveal all contaminants that could come from the extraction and other technical steps, and not from the sample itself.

Data preprocessing

After the acquisition, Bruker raw data .d files were automatically calibrated using the internal calibration and converted into mzXML format using a custom DataAnalysis script (Bruker, Version 4.3). The mzXML files were then subjected to the standard alignment and peak picking procedure using xcms software [21]. We then filtered from the output table all lipid features with the coefficient of variation (CoV, calculated as the standard deviation over the mean across QC samples) > 30%, and peaks with zero values in > 50% of

the individual samples. Lipid features' intensities were then normalized using the upper quartile normalization and base-two log-transformed. Raw data is uploaded to the metabolomics study data repository MetaboLights [22].

Phylogenetic distances calculation

The lipid intensity-based distances between species were calculated as the Euclidean distance between the vectors containing the intensities of 472 lipids detected in each pair of species. The phylogenetic distances between the species' pairs were obtained from the TimeTree database [23].

Statistical analysis

Species-dependent lipids were defined with ANOVA and BH-corrected p-value cutoff of 0.05. The correlation matrix of species-dependent lipids was calculated as (1-cor) Pearson's distances between all lipids. Unsupervised clustering of the species-dependent lipids was performed using hierarchical clustering with complete linkage in the R statistical environment.

TAGs annotation

All detected lipid features were annotated against the theoretical list with all possible masses of NH_4^+ adducts of TAGs. The theoretical list of masses was generated using ALEX Target List Generator with the ALEX lipid database (5.2) [24]. Among the detected lipids, 76 matched the theoretical masses with < 10 ppm and were considered for further analysis.

Species-dependent TAG intensity differences

We calculated the mean intensities of TAGs in each species using the raw intensities of the annotated TAGs. To assess TAGs concentrations in each species, the mean intensity of a particular TAG was divided by the sum of the mean intensities of all TAGs in that species. For comparison between species, the 100% intensity value of the TAG was defined as the maximal intensity of the TAG across the species.

Declarations

Ethics approval and consent to participate The study was carried out with the ethical approval of the Institutional Review Board of the Skolkovo Institute of Science and Technology (non-regular meeting No 2). All participants have signed an Informed Consent form.

Consent for publication*Not Applicable*

Availability of data and materials The datasets generated and analysed during the current study are available in the MetaboLights repository, www.ebi.ac.uk/metabolights/MTBLS1338.

Competing interests The authors declare that they have no competing interests.

Funding This work was supported by the Strategic Priority Research Program of the Chinese Academy of Sciences (grant XDB13010200); the National Natural Science Foundation of China (grant 31420103920);

the National One Thousand Foreign Experts Plan (grant WQ20123100078); the National Key R&D Program of China (grant 2017YFA0505700); and the Russian Science Foundation (grant 16-14-00220). Funding sources played no role in the study design, execution, analysis, data interpretation, or the writing of this manuscript.

Authors' contributions PK and WM conceived and designed the study. SG and AM organized samples collection. AV, NA, WM and AM performed samples preparation, lipid extraction and mass-spectrometry. PM and AM performed statistical analysis and contributed figures. PK and AM wrote the manuscript. All authors read and approved the final version of manuscript.

Acknowledgements We thank Peng Shi for providing yak milk samples; Vadim Bakushkin and Bulatovo Farm for their generous help in goat milk sample collection; Ksenia Fominykh and Svetlana Gribova for organising human milk samples collection; Markus R. Wenk and his team at the National University of Singapore for valuable comments and suggestions.

Additional files

Additional file 1: **Figure S1**. Mass spectrometry output showing 76 lipid features computationally annotated as TAGs. The x-axis shows the compounds' mass-by-charge ratio (m/z). The y-axis shows retention time (RT) of the compound on the liquid chromatography preceding mass spectrometry. Colors indicate four clusters of lipids showing intensity differences among species. Each point represents annotated TAG feature; labels include the cumulative length of the carbon chains and the total number of double bonds of the fatty acid residues.

Additional file 2: **Figure S1.** Mass spectrometry output showing 76 lipid features computationally annotated as TAGs. The x-axis shows the compounds' mass-by-charge ratio (m/z). The y-axis shows retention time (RT) of the compound on the liquid chromatography preceding mass spectrometry. Colors indicate two clusters of lipids showing intensity differences between humans and two macaque species. Each point represents annotated TAG feature; labels include the cumulative length of the carbon chains and the total number of double bonds of the fatty acid residues.

Additional file 3: **Figure S3.** Mass spectrometry output showing 76 lipid features computationally annotated as TAGs. The x-axis shows the compounds' mass-by-charge ratio (m/z). The y-axis shows retention time (RT) of the compound on the liquid chromatography preceding mass spectrometry. Colors indicate two clusters of lipids showing intensity differences between humans and bovid species (cows, yaks, goats). Each point represents annotated TAG feature; labels include the cumulative length of the carbon chains and the total number of double bonds of the fatty acid residues.

Additional file 4: **Figure S4.** Mass spectrometry output showing 76 lipid features computationally annotated as TAGs. The x-axis shows the compounds' mass-by-charge ratio (m/z). The y-axis shows retention time (RT) of the compound on the liquid chromatography preceding mass spectrometry. Colors indicate two clusters of lipids showing intensity differences between humans and pigs. Each point

represents annotated TAG feature; labels include the cumulative length of the carbon chains and the total number of double bonds of the fatty acid residues.

Additional file 5: **Table S1.** Data overview. Number of samples used in this study.

Additional file 6: **Table S2.** Computationally annotated TAG features. The feature annotation was based on m/z values of the intact ions and, therefore, informed about the cumulative length and unsaturation degree of three fatty acid residues.

Abbreviations

ANOVA - analysis of variance

BEH - bridged ethylene hybrid

BH - Benjamini-Hochberg

CoV - coefficient of variation

DHA - docosahexaenoic acid

LC-MS - liquid chromatography mass-spectrometry

LPC - lysophosphatidylcholine

MDS - multidimensional scaling

MeOH - methanol

MTBE - methyl tert-butyl ether

QC - quality control

QTOF - quadrupole-Time-of-Flight

RT - retention time

TAG - triacylglyceride

UPLC - ultra-performance liquid chromatography

References

1. Wu X, Jackson RT, Khan SA, Ahuja J, Pehrsson PR. Human Milk Nutrient Composition in the United States: Current Knowledge, Challenges, and Research Needs. Curr Dev Nutr. 2018; 2:nzy025.

2. Ballard O, Morrow AL. Human Milk Composition. Pediatric Clinics of North America. 2013; 60:49–74. doi: 10.1016/j.pcl.2012.10.002.
3. Hinde K, Milligan LA. Primate milk: proximate mechanisms and ultimate perspectives. Evol. Anthropol. 2011; 20:9–23.
4. Savino F, Petrucci E, Lupica MM, Nanni GE, Oggero R. Assay of ghrelin concentration in infant formulas and breast milk. World J. Gastroenterol. 2011; 17:1971–1975.
5. Bhinder G et al. Milk Fat Globule Membrane Supplementation in Formula Modulates the Neonatal Gut Microbiome and Normalizes Intestinal Development. Sci. Rep. 2017; 7:45274.
6. Hampel D, Shahab-Ferdows S, Islam MM, Peerson JM, Allen LH. Vitamin Concentrations in Human Milk Vary with Time within Feed, Circadian Rhythm, and Single-Dose Supplementation. J. Nutr. 2017; 147:603–611.
7. Innis SM. Dietary (n-3) Fatty Acids and Brain Development. The Journal of Nutrition. 2007; 137:855–859. doi: 10.1093/jn/137.4.855.
8. Mulder KA, Elango R, Innis SM. Fetal DHA inadequacy and the impact on child neurodevelopment: a follow-up of a randomised trial of maternal DHA supplementation in pregnancy. Br. J. Nutr. 2018; 119:271–279.
9. Oftedal OT, Bowen WD, Boness DJ. Energy Transfer by Lactating Hooded Seals and Nutrient Deposition in Their Pups during the Four Days from Birth to Weaning. Physiol. Zool. 1993; 66:412–436.
10. Power LM, Shulkin J. Milk: the biology of lactation. JHU Press; 2016. p. 120.
11. Walstra P. Dairy Technology: Principles of Milk Properties and Processes. CRC Press; 1999.
12. Morera S, Castellote AI, Jauregui O, Casals I, López-Sabater MC. Triacylglycerol markers of mature human milk. Eur. J. Clin. Nutr. 2003; 57:1621–1626.
13. Haddad I, Mozzon M, Strabbioli R, Frega NG. A comparative study of the composition of triacylglycerol molecular species in equine and human milks. Dairy Sci. Technol. 2012; 92:37–56.
14. Beccaria M et al. High performance characterization of triacylglycerols in milk and milk-related samples by liquid chromatography and mass spectrometry. J. Chromatogr. A. 2014; 1360:172–187.
15. Linderborg KM et al. Tandem mass spectrometric analysis of human milk triacylglycerols from normal weight and overweight mothers on different diets. Food Chem. 2014; 146:583–590.
16. Ten-Doménech I, Beltrán-Iturat E, Herrero-Martínez JM, Sancho-Llopis JV, Simó-Alfonso EF. Triacylglycerol Analysis in Human Milk and Other Mammalian Species: Small-Scale Sample Preparation, Characterization, and Statistical Classification Using HPLC-ELSD Profiles. Journal of Agricultural and Food Chemistry. 2015; 63:5761–5770. doi: 10.1021/acs.jafc.5b01158.
17. Liu Z, Cocks BG, Rochfort S. Comparison of Molecular Species Distribution of DHA-Containing Triacylglycerols in Milk and Different Infant Formulas by Liquid Chromatography–Mass Spectrometry. J. Agric. Food Chem. 2016; 64:2134–2144.

18. Nguyen LN et al. Mfsd2a is a transporter for the essential omega-3 fatty acid docosahexaenoic acid. Nature. 2014; 509:503–506.
19. Cimatti AG et al. Maternal Supplementation With Krill Oil During Breastfeeding and Long-Chain Polyunsaturated Fatty Acids (LCPUFAs) Composition of Human Milk: A Feasibility Study. Front Pediatr. 2018; 6:407.
20. Sarafian MH et al. Objective Set of Criteria for Optimization of Sample Preparation Procedures for Ultra-High Throughput Untargeted Blood Plasma Lipid Profiling by Ultra Performance Liquid Chromatography–Mass Spectrometry. Analytical Chemistry. 2014; 86:5766–5774. doi: 10.1021/ac500317c.
21. Smith CA, Want EJ, O'Maille G, Abagyan R, Siuzdak G. XCMS: processing mass spectrometry data for metabolite profiling using nonlinear peak alignment, matching, and identification. Anal. Chem. 2006; 78:779–787.
22. Haug K et al. MetaboLights - an open-access general-purpose repository for metabolomics studies and associated meta-data. Nucleic Acids Res. 2013; 41:D781–6.
23. Hedges B, Kumar S. TimeTree knowledge-base for information on the tree-of-life and its evolutionary timescale. http://timetree.org/ Accessed 9 April 2019.
24. Husen P et al. Analysis of Lipid Experiments (ALEX): A Software Framework for Analysis of High-Resolution Shotgun Lipidomics Data. PLoS ONE. 2013; 8:e79736. doi: 10.1371/journal.pone.0079736.

Figures

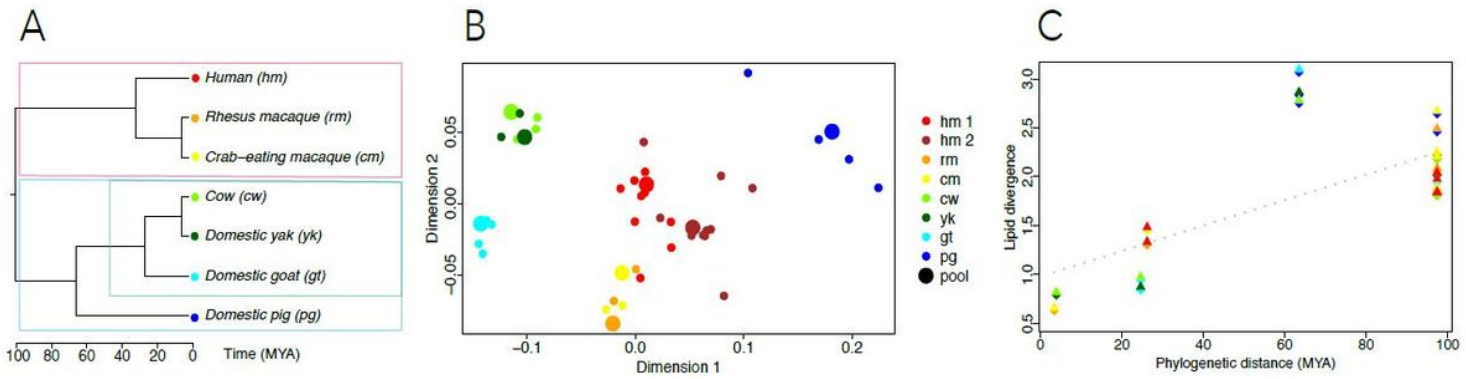

Figure 1

Milk lipidome evolution. (A) Dendrogram showing the phylogenetic relationship among seven mammalian species used in the study. Colored dots indicate species, with colors used consistently throughout figures. Colored frames indicate three groups: primate (red), artiodactyla (blue), and bovidae (green). (B) The relationship among milk samples based on the signal intensities of 472 detected lipid

features plotted in two dimensions using a multidimensional scaling algorithm. Colors represent species. Small dots represent individual milk samples. Large dots represent pools of samples from one species. (C) The relationship between lipid-intensity-based distances between species pairs and phylogenetic distances.

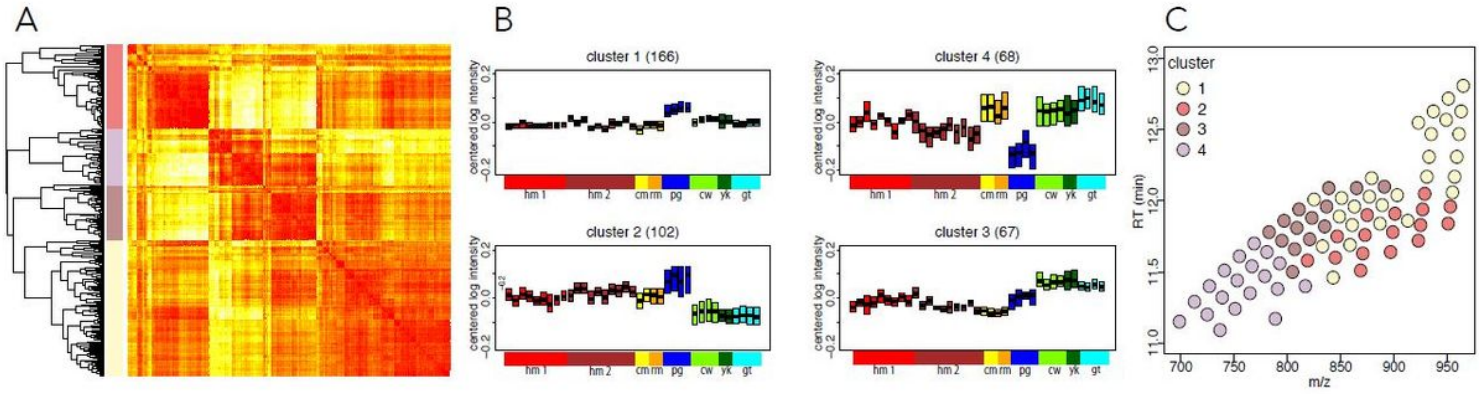

Figure 2

Patterns of lipid composition differences among species. (A) Unsupervised hierarchical clustering dendrogram and heatmap based on pairwise correlation-based distances between lipid intensity vectors. Color bar indicates four major lipid clusters: cluster 1 – yellow, cluster 2 – pink, cluster 3 – brown, cluster 4 – gray. (B) Distribution of centered lipid intensities in each cluster. Each box represents the interquartile distribution of lipid intensities in a sample. The number of lipids contained in a cluster is shown at the top of the panels. Samples colored and ordered by species. (C) Mass spectrometry output showing 76 computationally annotated TAGs colored by clusters. The x-axis shows the compounds' mass-by-charge ratio (m/z). The y-axis shows retention time (RT) of the compound on the liquid chromatography preceding mass spectrometry.

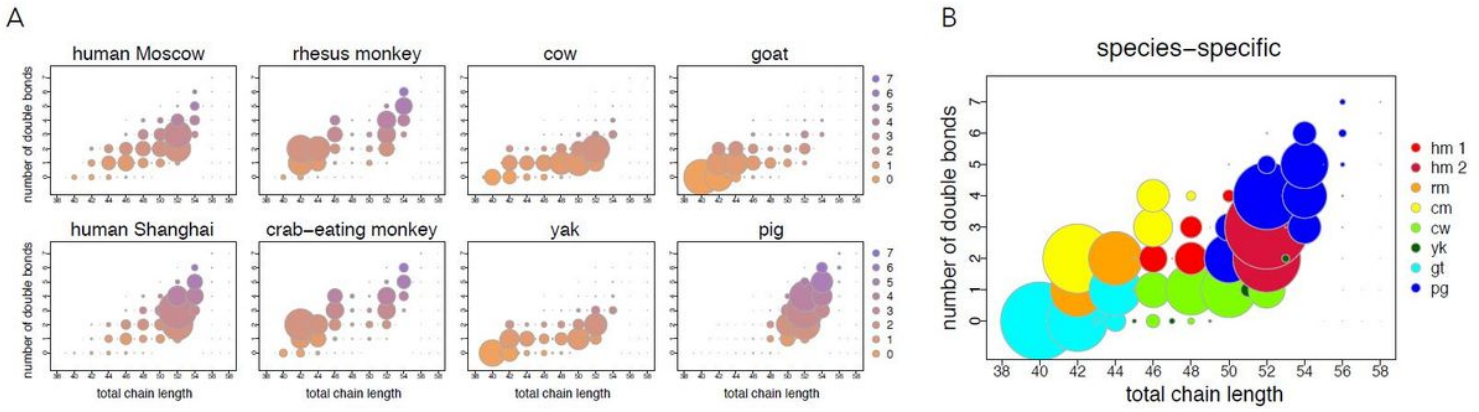

Figure 3

Breast milk TAG repertoire in each species. (A) Distribution of breast milk TAGs in each species and two human populations. The x-axis represents the total chain length of three TAG fatty acid residues. The y-axis represents the number of double bonds in TAG fatty acid residues. The size of the circles represents

TAG intensity calculated as the mean intensity of the TAG in a species divided by the sum of the mean intensities of all TAGs in this species. Colors represent the number of double bonds with a gradient from orange – zero double bonds to purple – seven double bonds. (B) Cumulative distribution of species-specific TAGs features. The axes as in panel A. Size of the circles represents the maximum intensity of a TAG across species. Colors indicate species with the maximum intensity of a TAG.

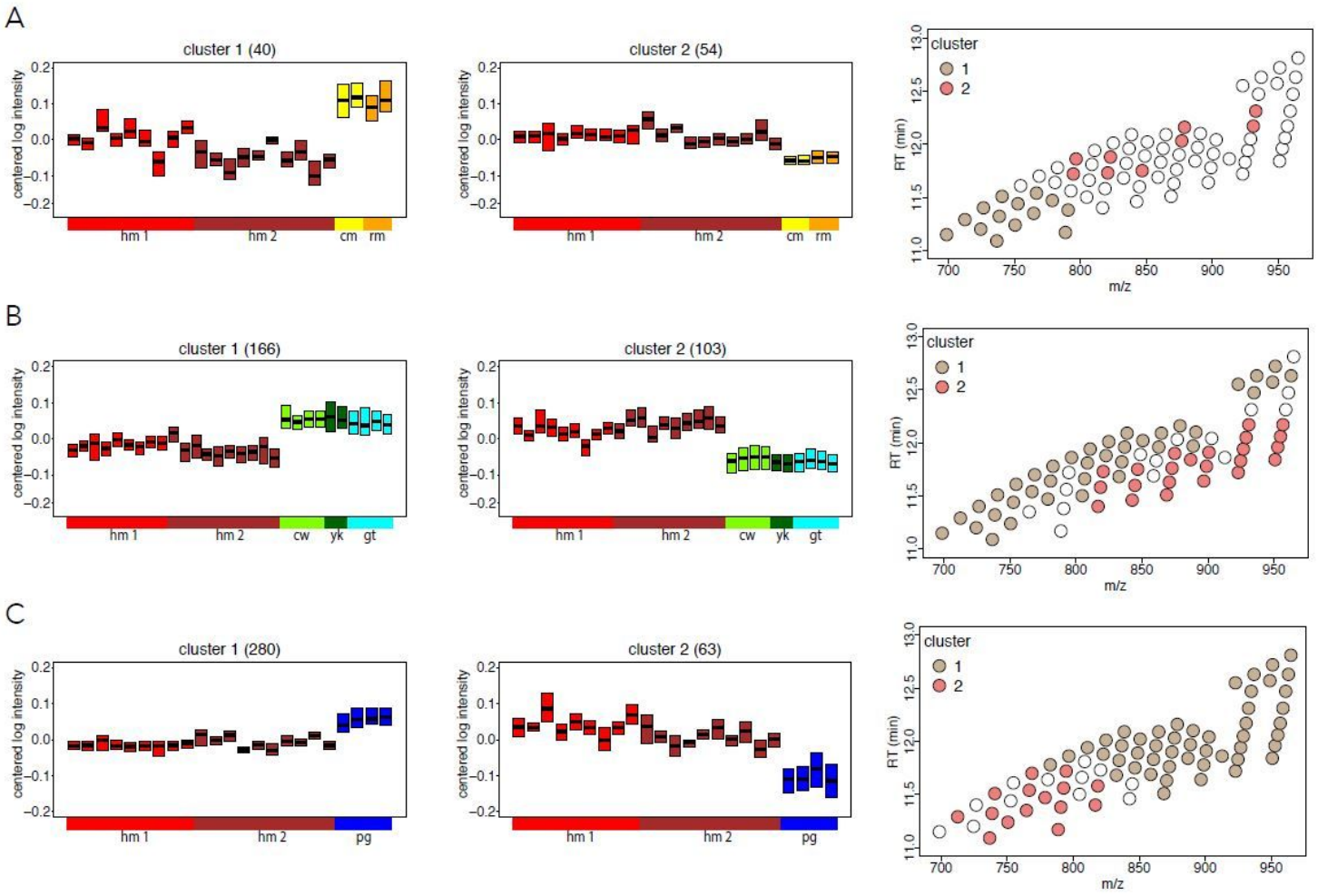

Figure 4

Comparison of breast milk TAG profiles between humans and other species. (A) Left: Distribution of centered intensities of 94 lipids showing differences between humans and two macaque species separated into two clusters. Each box represents the interquartile distribution of lipid intensities in a sample. The number of lipids contained in a cluster is shown at the top of the panels. Samples colored and ordered by species. Right: Mass spectrometry output with 76 computationally annotated TAGs showing the difference between humans and two macaque species colored by clusters. (B) As panel A, for 76 lipids showing intensity differences between humans and three bovidae species. (C) As panel A, for 76 lipids showing intensity differences between humans and pigs.

Supplementary Files

This is a list of supplementary files associated with this preprint. Click to download.

- Additionalfile3.pdf
- Additionalfile1.pdf
- Additionalfile2.pdf
- Additionalfile4.pdf
- Additionalfile6.pdf
- Additionalfile5.pdf